NLR-TP-2002-305

Experimental and theoretical assessment of the helicopter ground vortex phenomenon

J.F. Boer, C. Hermans and K. Pengel (DNW)

NLR-TP-2002-305

Experimental and theoretical assessment of the helicopter ground vortex phenomenon

J.F. Boer, C. Hermans and K. Pengel (DNW)

This report is based on a presentation held at the CEAS - TRA3 Conference on 10-12 June 2002, Cambridge, UK.

Contents

(14 pages in total)

Abbreviations

BLC	Boundary Layer Control
CIRA	Italian Aerospace Research Centre
DERA	Defence Evaluation and Research Agency
DLR	German Aerospace Centre
DNW	German-Dutch Wind Tunnels
LLF	Large Low-speed Facility
LLS	Laser Light Sheet
MWM	Modular Wind tunnel Model
NLR	National Aerospace Laboratory NLR
NTUA	National Technical University Athens
ONERA	French National Aerospace Research Establishment
PIV	Particle Image Velocimetry
TUBS	Technical University of Braunschweig

Notations

C_T	Rotor thrust co-efficient
D	Rotor diameter
H	Rotor height above ground
R	Rotor radius
S	Horizontal position in measurement or calculation plane
V_{fwd}	Helicopter forward speed
V_{tip}	Rotor tip speed
X	Horizontal position along the helicopter plane of symmetry
Z	Height above ground
μ	Advance ratio (helicopter forward speed / rotor tip speed)

Experimental and Theoretical Assessment of the Helicopter Ground Vortex Phenomenon

J.F.Boer, C. Hermans
National Aerospace Laboratory NLR
Amsterdam, The Netherlands

K. Pengel
German-Dutch Wind Tunnels DNW
Emmeloord, The Netherlands

Abstract

During recent wind tunnel tests, performed in the European 4th Framework program HELIFLOW, the position and flow characteristics of the rotorwash-induced ground vortex were measured. These results were used for the verification and improvement of the NLR helicopter ground vortex calculation model, which is part of the rotorwash induced horizontal airflow calculation tool OUTWASH, currently under development for the Ministry of Defence of the Netherlands.

The wind tunnel tests were performed in the Large Low-speed Facility of the German-Dutch Wind Tunnels. The use of state-of-the-art test techniques, such as Laser Light Sheet and Particle Image Velocimetry, and DLR's powered main rotor BO 105 wind tunnel model made it possible to measure the ground vortex induced velocities.

The NLR ground vortex mathematical model is a tool for the prediction of the helicopter ground vortex position, shape and strength. It consists of an empirical radial wall-jet model and a set of airflow equilibrium equations. The vortex is represented by discrete filaments, while the induced velocities are calculated using Biot Savart law.

The improved ground vortex model calculation results show a good match with the experimental ground vortex core positions and strengths data for all HELIFLOW test conditions.

Introduction

The helicopter ground vortex is a horseshoe shaped vortex originating in front of the helicopter and trailing downwind along both edges of the rotor disk. The phenomenon occurs for helicopters flying low above the ground with slow forward speed or in a hover in wind condition. The work presented in this paper contains an experimental and a theoretical part.

Experimental

The experimental work was undertaken as part of the Brite Euram project HELIFLOW (Ref. 1).

Project members were Agusta, CIRA, QinetiQ (former DERA), DLR, Eurocopter, Eurocopter Deutschland, Westland Helicopters, NLR, NTUA, ONERA and TUBS. DNW acted as subcontractor.

Two of the aims of the HELIFLOW project were to:
- clarify the usefulness of today's state of the art wind tunnel test techniques as a tool to study wake interaction phenomena, and
- study theoretical wake model prediction capabilities for these complex conditions.

Task 3 of the HELIFLOW project addressed the low speed phenomena during sideward and quartering flight. During these flight conditions in ground proximity various wake interference phenomena occur. The ground vortex induced by the helicopter main rotor influences the main and tail rotor inflow conditions and thus its performance. These adverse flight conditions confront the pilot with increased workload due to fluctuations in power required, available tail rotor thrust and thus control margin.

Since these problems mainly deal with interactional aerodynamics of complex wake structures, they are difficult to address on small-scale models in a wind tunnel environment and challenging to predict.

The experimental assessment of the ground vortex was performed by conducting wind tunnel tests with the DLR BO 105 (1/2.5-scale) powered model in the Large Low-speed Facility (LLF) of the German-Dutch Wind Tunnels (DNW), see figure 1.

Figure 1 BO 105 model in DNW-LLF test section

State of the art airflow test techniques were applied by DNW to measure the structure of the ground vortex. The NLR performed analysis of the ground vortex test results.

Theoretical

The theoretical part of the work presented was performed partly in the HELIFLOW-project, but mainly under a contract awarded by the Co-ordinator Spatial Planning and Environment of the Ministry of Defence of The Netherlands, which ministry also finances the NLR in-house development of the rotor outwash calculation tool OUTWASH (Ref. 2 & 3).

The OUTWASH code is an MS-Windows based object oriented code developed in Borland Delphi. It contains several characteristic aerodynamic models, including a ground vortex position and identification model.

Outwash is the horizontal airflow over the ground caused by the rotor downwash of very low flying helicopters. The presence of the ground bends the vertical downwash into a horizontal outwash. This outwash affects a much larger area than the vertical downwash does.

The aim of the Outwash-project is to determine:
- the magnitude of the outwash airflow velocities induced by low flying helicopters;
- the area affected by helicopter outwash.

The theoretical assessment of the ground vortex was performed by comparison of the OUTWASH predicted ground vortex with the HELIFLOW wind tunnel test results. NLR determined aerodynamic relations and performed parameter sensitivity analyses to develop the improved empirical relations for the ground vortex position and identification model.

Purpose

The long-term purpose of these research items is the availability of advanced and reliable experimental and theoretical methods in rotorcraft interactional aerodynamics. This will contribute to:
- reduced development cost of future helicopter designs through the ability to better predict the behaviour of the aircraft before flying it;
- improved operational, but still safe capabilities through a better knowledge of the flying characteristics of the helicopter;
- improved operational safety due to a better knowledge of helicopter outwash hazards;
- improved knowledge of the eventual environmental burden of outwash on military training areas.

Wind tunnel tests

Pre-test calculations

Initial BO 105 main rotor ground vortex calculations have been performed with the NLR OUTWASH-code for a large number of conditions (Ref. 4), including those defined in the preliminary wind tunnel test matrix. Calculations were performed for forward (equivalent to sideward) flight, and hover in wind case (for equal relative airspeeds), since, due to the differences in boundary layer profiles, the ground vortex develops in a different way.

Numerical results showed that for hover in wind, the ground vortex develops later (i.e. at higher wind speeds), is wider in size and exists over a larger range of relative airspeeds as compared to the forward flight case. The significance of these differences led to the decision to apply Boundary Layer Control (BLC) by means of tangential air blowing during the wind tunnel campaign. In this way sideward flight conditions in-ground effect could be reproduced more realistically.

The initial ground vortex calculations also showed the sensitivity of the flow conditions to changes in tunnel speed and model height above ground. The results were used to refine the preliminary wind tunnel test matrix in terms of relevant wind tunnel test speeds and model height settings above ground. Furthermore, it allowed the experimental set-up for the measurements to be precised such that without changing the measurement equipment set-up, all ground vortex measurements could be conducted.

Figure 2 shows the vertical plane (indicated as Laser Light Sheet) in which the ground vortex cross flow components were measured. The measurement results include the ground vortex core location and the velocity distribution in the measurement plane.
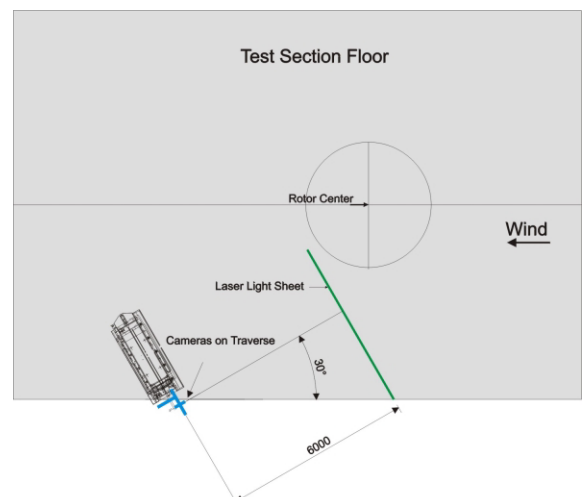

Figure 2 Location of measurement plane

Test set-up

The wind tunnel model consisted of a powered 4-bladed main and 2-bladed tail rotor, drive & blade control systems, fuselage, 6-component rotor and fuselage balances and rotor sensors. The main rotor used is a 40%-geometrically and dynamically scaled, hingeless BO 105 rotor. The rotor system was mounted on DLR's Modular Wind tunnel Model (MWM) and driven by a 130 kW hydraulic motor. The model was mounted on a vertical sting support system, allowing adjustment of the rotor height above ground.

The model was operated at the equivalent full-scale nominal thrust level and tip Mach number. During the ground vortex measurement part of the test campaign, the main rotor was trimmed for zero blade flapping. The tail rotor was not operated.

In order to minimise the wind tunnel wall interference effects it was decided to use the 9.5 * 9.5 m test section of DNW-LLF in the open jet configuration (so-called ¾ open test section). To stabilise the flow, even at the relatively low wind speeds for the sideward flight tests (< 18 m/s), Seifert winglets were mounted at the wind tunnel nozzle to avoid low frequency pressure waves.

The boundary layer over the wind tunnel floor was minimised by using the Boundary Layer Control (BLC) system. It blows a high-energy tangential air jet (2.4 kg/s) through a 1.0 mm slot (6 m width) in the wind tunnel floor upstream of the model into the wind tunnel boundary layer.

The test set-up in the three-quarter open test section of the DNW-LLF is presented in figure 3 (Ref. 5).
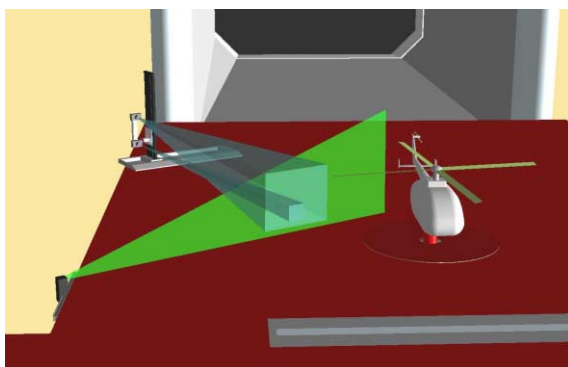

Figure 3 Test set-up in ¾ open test section

State of the art airflow test techniques were applied like Laser Light Sheet (LLS) and Particle Image Velocimetry (PIV) to measure the specific flow characteristics of the ground vortex on the advancing rotor side. The Nd-YAG-II laser heads (Quantel Brilliant B type) with pulse energy of 350 mJ were located on the ground of the testing hall. The emitted beam was led to the light sheet generating optics by means of mirrors. This optical device was mounted at the edge of the test section floor. A mirror at the end of the optics directed the laser light sheet to the defined measuring location.

The flow was seeded in the settling chamber. The seeding rake (2.5 x 2.0 m) was connected to two seeding generators, equipped with Laskin nozzles to produce an aerosol of an adjustable particle size. The generated particles were droplets of about 1 μm in size. Di-2-Ethylhexyl-Sebacat (DEHS) was used as liquid. Due to the contraction of the flow in the nozzle the actual seeded circular area had a diameter of approximately 0.5 m.

Two PCO Sensicam double image cameras, which could be triggered externally, were used to record the PIV and LLS images. Both cameras were mounted on the same traversing system with the line-of-sight normal to the light sheet.

Measurement method

The size of the LLS image was 1.4 by 1.1 m^2. The PIV image size was 0.4 by 0.32 m^2. The camera resolution was 1280x1024 pixels. Each camera took three image pairs per second.

The PIV images were taken in double frames / single exposure mode, which made it possible to determine the velocity distribution by means of image cross correlation. The LLS images also were taken in the double frames / single exposure mode, which made it possible to correlate LLS image pairs by means of PIV correlation software as well.

A correlation of the LLS images led to meaningful velocities and vortex core positions, which have been validated by means of PIV image results. The PIV correlation software determines displacements of single seeding particles by correlating the PIV image pairs. With the displacement (direction and magnitude) and the separation period between the two images a velocity vector is calculated. However, the resolution of the LLS images (1.4 mm/pixel) is much lower than the PIV image resolution (0.3 mm/pixel). This resolution makes it unlikely that single seeding particles will be recognised within the LLS images. Within the PIV images the light spot of one single particle illuminates about 2 to 3 pixel so that there is a clear contrast to the dark background. Within a LLS image, which resolution is more than four times lower, less than one pixel would be illuminated. I.e. there is only a low contrast of one pixel to the background and the PIV correlation software is not likely to detect this low-contrast pixel as seeding particle. However, the correlated LLS image pairs showed meaningful results. An explanation for this is, that the software correlates

groups of particles, groups, which do not change their shape from one image to the other and which behaviour is similar to single particles.

All PIV double-images were evaluated with a 32 pixel by 32-pixel sampling-window size, using 50% overlapping. Achieved velocity vector accuracy was 1.0 m/s.

The LLS double-images were evaluated with a 64 pixel by 64-pixel sampling-window size and a 128 pixel by 128-pixel sampling-window size, both using 32-pixel overlapping (respectively 50% and 25% overlapping. Achieved velocity vector accuracy for LLS was 4.4 m/s. The 64 pixel windows were used to determine the ground vortex vorticity and the 128-pixel windows were used to determine the vortex core positions.

During wind tunnel testing, the LLS acquired velocity vector map images were mainly used to localise the vortex core position. The vortex structure could be recognised by averaging the 36 instantaneous vector maps of each measurement sequence. In addition, PIV images were taken in the vortex core area to precisely measure local flow conditions.

Analysis of results
Correlation of the LLS vector maps with the PIV vector maps resulted in the same vortex core position considering the spatial resolution of the

LLS vector maps. Since the validated LLS vector maps cover a larger area of the measurement plane, LLS vector maps were used for the further analysis of the test results. Sample LLS and PIV average vector maps are shown in figure 4 (Ref. 6). The arrow greyscales and lengths indicate the magnitude of local airflow velocities (with different (grey)scales for PIV and LLS).

Table 1 lists the DNW test conditions where a clear vortex structure in the LLS measurement plane was identified and for which comparative OUTWASH calculations were performed.

Table 1 Test conditions with a vortex structure

DNW run	WT-speed [m/s]	Z_{rotor} [m]	Z_{rotor}/R [-]	Outwash
1002	10.9	1.48	0.74	101
1003	10.9	1.68	0.84	102
1004	10.8	1.88	0.94	103
1005	10.8	2.08	1.04	104
1105	10.7	2.28	1.14	105
1101	11.0	1.28	0.64	106
1010	11.0	1.48	0.74	107
1009	9.9	1.48	0.74	108
1007	7.6	1.48	0.74	109
1012	13.0	1.48	0.74	110

First the vortex core positions have been determined for the measurement runs given in table 1.
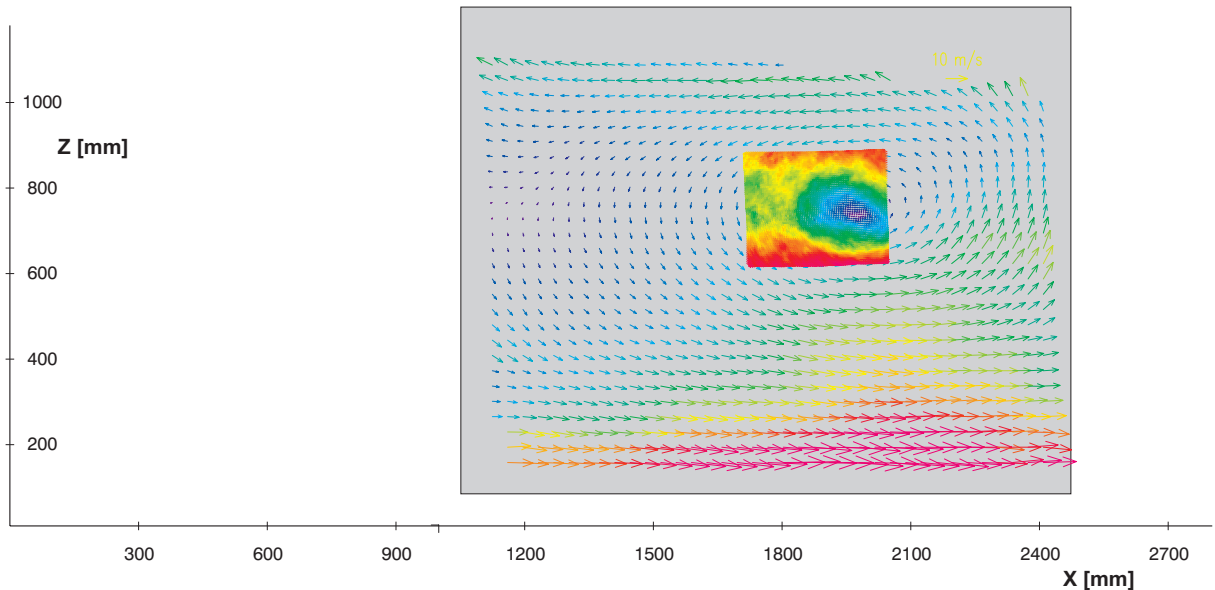

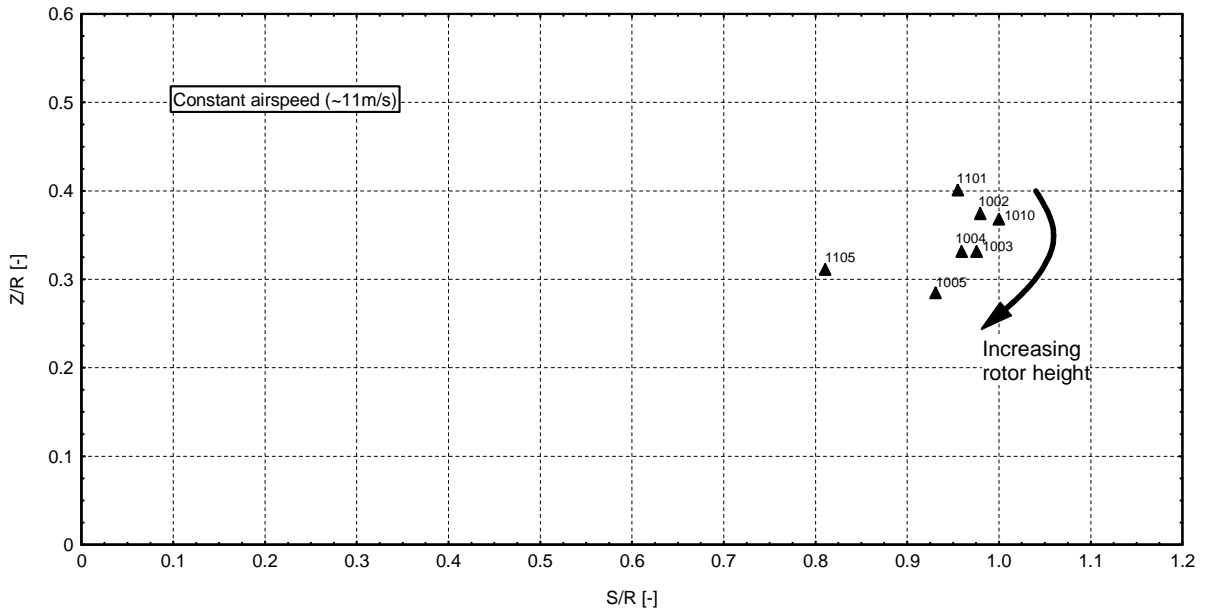*Figure 4 Ground vortex LLS and PIV average vector maps*

Figure 5 Measured ground vortex core positions in LLS-plane for various rotor heights

In figure 5 and 6 (Ref. 6) respectively, the effect of rotor height above ground and tunnel speed on the vortex core positions is shown. On the vertical axis the vortex core height above ground is indicated, on the horizontal axis the distance from the origin of the measurement plane is given. The origin is defined at the lower left corner of the LLS measurement plane.

Changing the rotor height above ground from 0.64 R (run no. 1101) to 1.04 R (run no. 1005) causes the ground vortex core to move downward. Changing

the rotor height further to 1.14 R (run no. 1105) does not move the vortex core more downward, but clearly moves the centre of the vortex core to the left. At lower rotor heights, apparently the presence of the fuselage prevents the ground vortex from moving downstream under the rotor. This could explain the limited horizontal movement (in the measurement plane) of the vortex core with changing rotor height. Further investigation into this effect is needed.
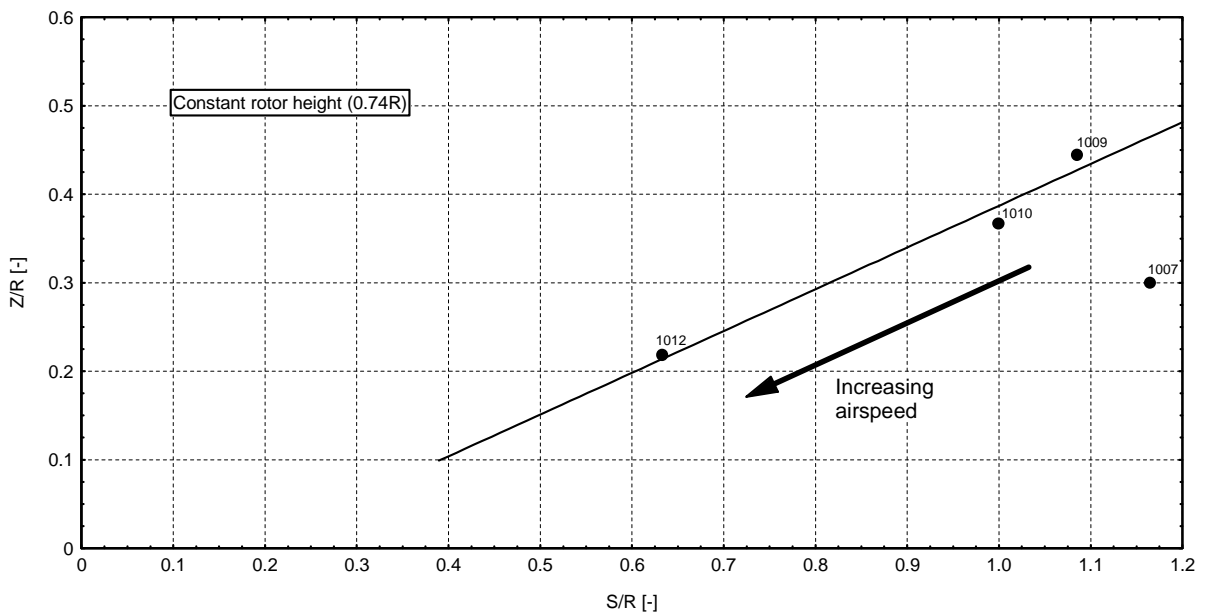

Figure 6 Measured ground vortex core positions in LLS-plane for various airspeeds

Reducing the tunnel speed at a constant rotor height above ground (0.74 R) from 13 m/sec (run no. 1012) to 9.9 m/sec (run no 1009) causes the vortex core to move along an almost straight line in an upward direction to the right. An interesting measurement point is the vortex core position at a speed of 7.6 m/s (run no. 1007). At this relatively low speed, the vortex core clearly moves downward. Further investigation into this effect is also needed. The ground vortex core position in the measurement plane is clearly much more sensitive to airspeed variations than to the rotor height variations under consideration.

The influence of the boundary layer thickness on the ground vortex structure was assessed using a Boundary Layer Control (BLC) system. By means of the so-called tangential blowing it was possible to vary the boundary layer thickness between 20 and 80 mm (measured at the centre of the test section). For one test condition, the tangential blowing was switched off (boundary layer thickness of 80 mm). The effect of this difference in boundary layer thickness appeared to be small with respect to the vortex core position changes in the measurement plane due to variation of rotor height and tunnel speed variation.

Secondly, the vortex strength has been determined from the measured LLS vector maps.

In figure 7 and 8 respectively, the effect of rotor height above ground and tunnel speed on the vortex strength is shown. On the vertical axis the vortex strength is indicated, on the horizontal axis respectively the dimensionless rotor height above ground and the advance ratio are given.
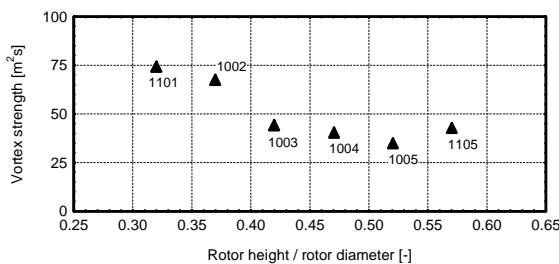

Figure 7 Measured ground vortex strength for varied rotor height

Increasing the rotor height above ground from 0.64 R (run no. 1101) to 1.04 R (run no. 1005) causes the ground vortex strength to decrease. Increasing the rotor height further to 1.14 R (run no. 1105) slightly increases the vortex strength again. The effect of decreasing vortex strength with increasing rotor height above ground can be explained by the movement of the vortex core more towards and immerged in the rotorwash. However, at the height

where the fuselage gives room for the vortex to move further backwards, the strength slightly increases again. Apparently, the presence of the fuselage has a (slightly) decreasing effect on the vortex strength.
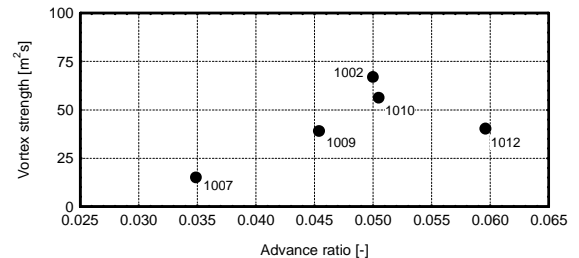

Figure 8 Measured ground vortex strength for varied air velocities

Increasing the tunnel speed at a constant rotor height above ground (0.74 R) from 7.6 m/sec (run no. 1007) to 11 m/sec (run no. 1010) causes the vortex strength to increase progressively. However, a further increase in tunnel speed to 13 m/s (run no. 1012) shows a decrease in vortex strength. The first increase with tunnel speed can be explained from the increase in interaction of the vortex with the rotor downwash as the vortex is pushed more towards the rotor downwash. Apparently, a further movement towards the (obstructing) fuselage will decrease the vortex strength. The vortex strength appears to be very sensitive to the tunnel speed variations.

The OUTWASH code

Application
The OUTWASH code can be used to calculate:
- an outwash footprint, i.e. a stationary outwash flow field close to the helicopter, as well as
- the resulting change of outwash with time caused by a fly-by of a low flying helicopter.

Calculations can be performed for both single main rotor and tandem rotor helicopters (adaptation for tilt rotor aircraft is possible). Typical calculation time for a ground vortex flow field on a PC is in the order of a minute, depending on the grid size.

To apply the code for the HELIFLOW Task 3 activities, the OUTWASH code has been extended with a model for the displacement effect of the rotorwash and the presentation of vertical velocities induced by the ground vortex. To enable the direct comparison of experimental results with numerical predictions, the capability to calculate induced velocities in a randomly positioned vertical plane in the area of interest was added. Figure 9 presents an example of the OUTWASH calculation results.
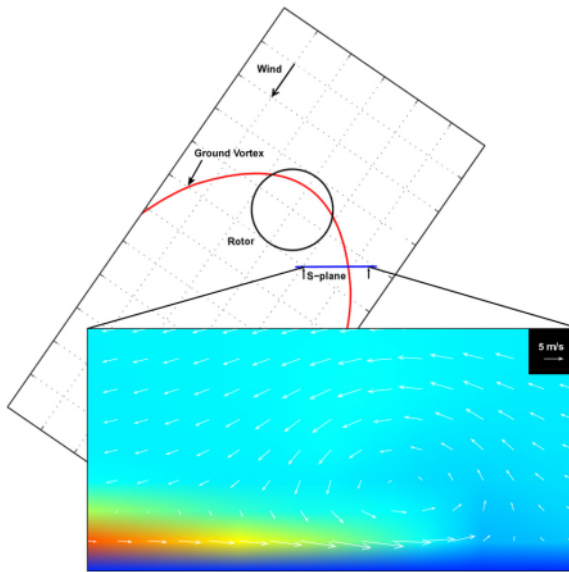
Figure 9   OUTWASH calculated ground vortex

Some additional data export features were also implemented to facilitate the production of the necessary figures. Reference 4 describes in more detail the code adaptations made.

Models and methods
The OUTWASH-code has a modular structure and consists of various models and methods. Based on the flight condition, a calculation method is selected, which will use one or more characteristic aerodynamic models to calculate the outwash flow field.
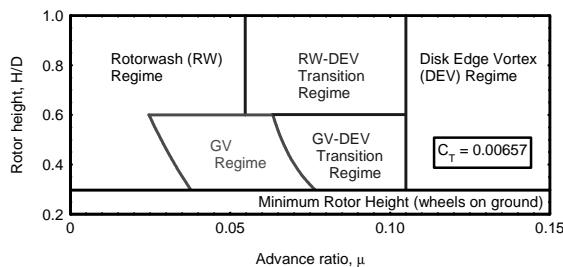

Figure 10 OUTWASH flight condition regimes

Distinction is made between the following flight condition regimes, see figure 10:
1. Hover and (very) slow forward flight or hover in moderate wind (hover / recirculation regime).
2. Slow forward flight (about 9m/s < V_{fwd} < 13m/s) or hover in wind, in ground effect (ground vortex regime).
3. Slow forward flight (about 9m/s < V_{fwd} < 13m/s) or hover in wind, out of ground effect.
4. Forward flight at moderate speeds (about 13m/s < V_{fwd} < 18m/s) or a combination of forward speed and wind (transition regime).
5. Forward flight at higher speeds (V_{fwd} > 18m/s) (trailing vortices regime).

Depending on the flight condition regime, one of the following calculation methods is selected:
• Rotorwash;
• Ground Vortex;
• Transition;
• Disk Edge Vortices.

These methods use, sometimes iteratively, one or more characteristic aerodynamic models. The code contains three main models and several supporting models. The main models are:
• *Radial wall-jet*
  An empirically radial wall-jet model to calculate the horizontal outflow caused by the rotorwash (Ref. 2 & 7).
• *Vortex*
  A free vortex wake model to calculate developed vortices and the induced flow velocities using the Biot-Savard law on the discrete filaments of the vortices (Ref. 2 & 3).
• *Ground Vortex Position*
  An empirically ground vortex position and identification model to calculate the position, shape and strength of the ground vortex (Ref. 3, and 8-10).

The ground vortex method, which uses all main characteristic aerodynamic models, was used for comparative calculations with the measured wind tunnel data. The Ground Vortex Position model was later on improved after analysis of the compared calculation and wind tunnel results.

Ground Vortex Position Model
The Ground Vortex position and identification model calculates the ground vortex position and shape using airflow equilibrium. The model assumes a parabolic shape of the ground vortex part in front of the helicopter. Starting with this generic shape, first the airflow equilibrium in the most forward point of the ground vortex, the ground vortex tip, is calculated, see figure 11. The equilibrium is determined from the resulting helicopter speed and wind speed vector, and the outwash airflow. The latter is calculated with the Radial wall-jet model.
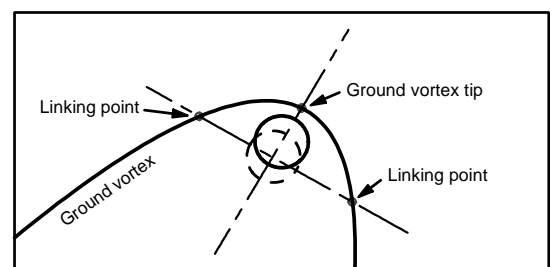

Figure 11 Ground vortex tip and linking points

Once the forward position of the ground vortex is known, the width of the ground vortex is calculated using the airflow equilibrium to the sides of the main rotor (linking point). This equilibrium defines the shape of the forward part of the ground vortex. At that point the parabola stops and is linked to the (free) trailing vortices. The trailing vortices are calculated with the Disk Edge Vortex model.

The set of equilibrium equations also contains the equations to calculate the ground vortex strength. The calculation of the ground vortex position, and shape is an iterative process, since it requires the ground vortex induced velocities.

The equilibrium equations have been empirically tuned to match measurement data from tests performed at Princeton University (Ref. 3, 8-10). These tests have been performed with an isolated rotor model in their former long track facility.

Post-test calculations and analysis
The original OUTWASH code has been applied for post-test calculations. Calculations were performed for the actual model configuration settings and wind tunnel conditions (tunnel speed, rotor thrust, rotor height above ground, boundary layer thickness). To include all measured conditions, the OUTWASH ground vortex method range was extended slightly in height (from H/D < 0.5 to H/D < 0.6) and speed. Figure 12 shows the measured conditions where a clear vortex structure in the LLS measurement plane was identified and the (adapted) speed boundaries for the ground vortex regime as used in the code.

Figure 13 shows the results of both the wind tunnel measurements and the OUTWASH calculations. The

calculations show a less wide vortex structure, resulting in vortex core positions closer to the origin of the measurement plane. Some conditions could not be reproduced, since according to the model the ground vortex already was "washed away" behind the rotor.
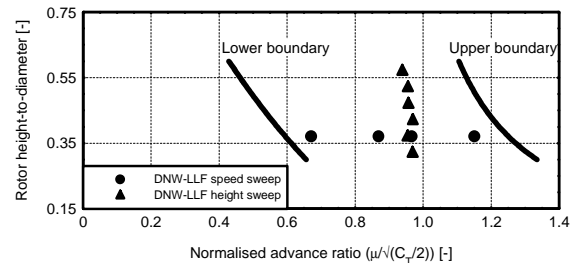

Figure 12 Ground vortex method flow regime

The differences between the calculation and experimental results are likely to be caused by the fact that the OUTWASH ground vortex model was tuned to isolated rotor measurement data, at the time of development the only reference data available. However, especially when operating very close to the ground, a displacement effect of the fuselage can be expected. It forces the ground vortex to stay well in front and aside of the fuselage. This could explain the differences in position along the S-axis.

It should be noted that the ground vortex position and shape is rather sensitive to the tunnel speed. A small change in the position and shape of the ground vortex frontal part leads to a relative large displacement of the vortex core position in the defined measurement/calculation plane. A change in
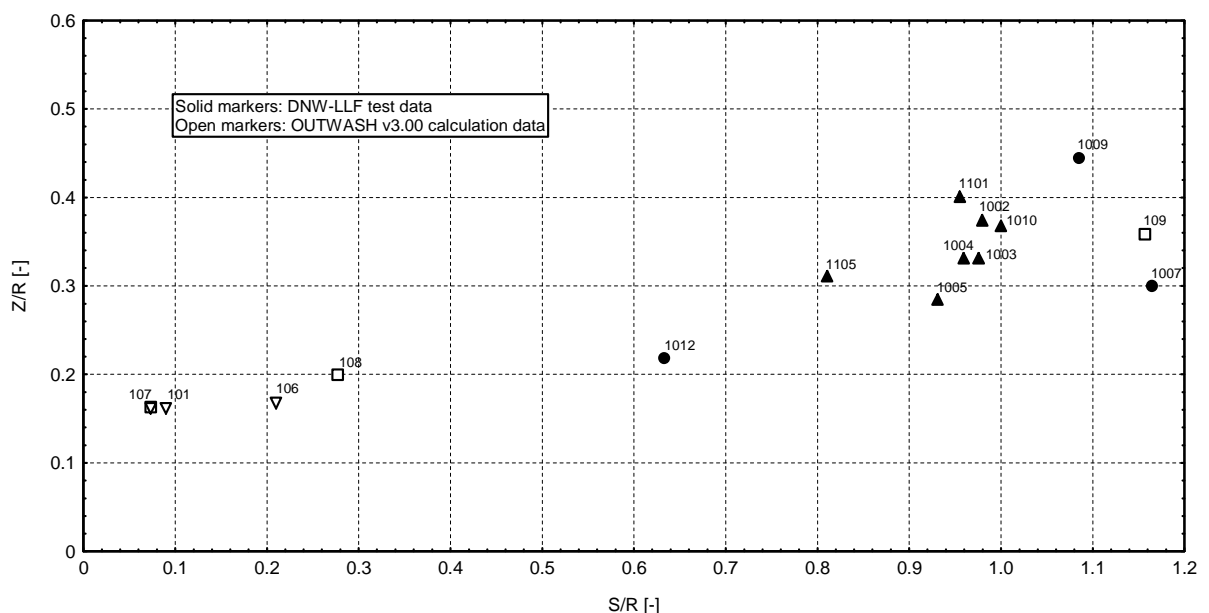

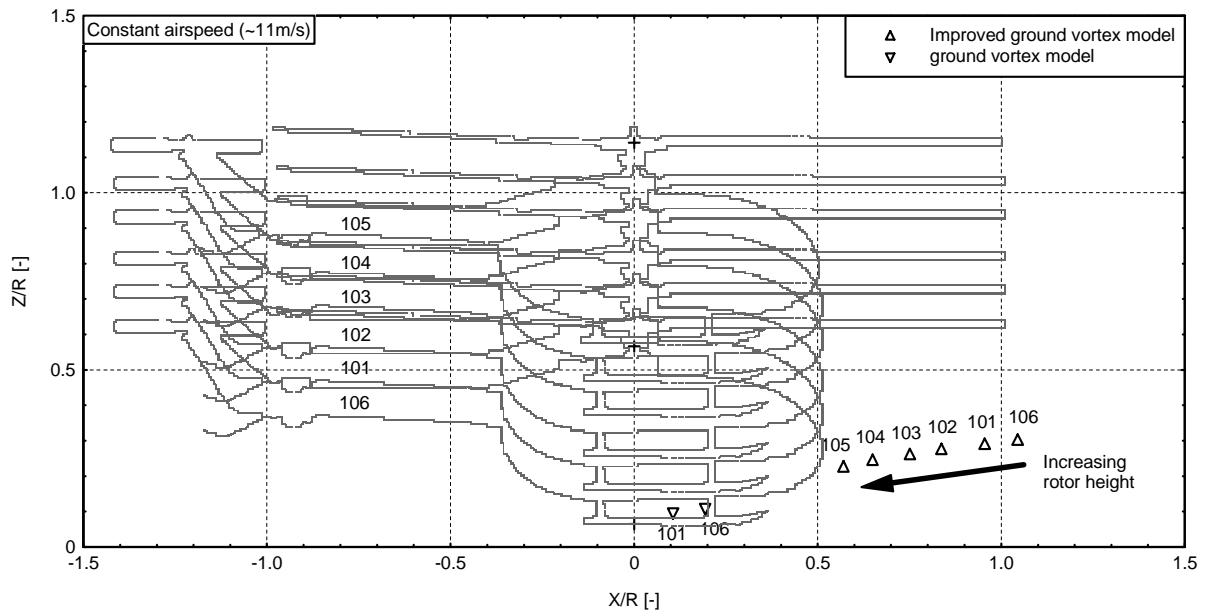*Figure 13 Comparison between OUTWASH (pre-test settings) and experimental results*

Figure 14 Calculated ground vortex tip positions and fuselage positions for various rotor heights

tunnel speed therefore has a relatively large effect on the vortex core position in the measurement plane.

The differences in height are likely caused by the effect of the rotorwash on the vortex tip. In the case of the isolated rotor OUTWASH calculations, the ground vortex moves downstream under the rotor into the rotorwash. The rotorwash pushes the ground vortex tip downwards, resulting in a lower vortex core height as compared to the DNW-LLF test results, where a fuselage was present and the ground vortex was not totally immersed in the rotorwash.

Model improvements
To analyse the fuselage displacement effect in more detail, ground vortex tip positions were calculated and plotted together with the helicopter fuselage, see

figure 14 and 15. The original ground vortex tip core positions appear unlikely close to the fuselage for most conditions. The fuselage probably will prevent the ground vortex from moving to that position.

The OUTWASH ground vortex position model has been improved by limiting the ground vortex tip position to the transition point, where the vertical downwash is bent into horizontal outwash. The ground vortex tip position will still be calculated based on equilibrium, but cannot move further backwards than the transition point.

Re-calculation of the ground vortex core positions in the HELIFLOW measurement plane resulted in a considerable improvement in the match between calculation and measurement data.
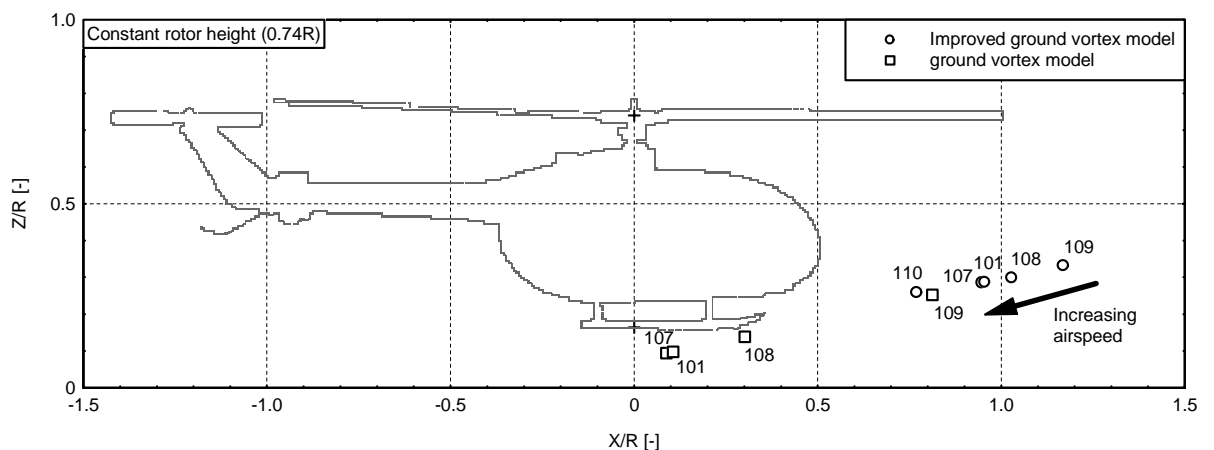

Figure 15 Calculated ground vortex tip positions and fuselage positions for various airspeeds

The inclusion of the displacement effect of the fuselage enabled tuning the equilibrium equations to match the wind tunnel test data. This involved the ground vortex horizontal and vertical linking point position as well as the ground vortex strength. After a parameter sensitivity study, one set of ground vortex model tuning parameters could be defined to match the BO 105 model ground vortex core positions for a wide range of conditions.

Calculation results
With the improved ground vortex model, the OUTWASH code was again applied to the actual HELIFLOW wind tunnel test conditions. Figure 16 shows the comparative results between the measurements and the OUTWASH calculations.

The calculations show a very good match for the horizontal ground vortex core position for all measurement conditions. The calculated vertical core positions seem to be less sensitive to rotor height and air velocity as compared to the wind tunnel test data.

Figure 17 and 18 respectively show the comparative results for the ground vortex strength with the dimensionless rotor height above ground and the advance ratio. The figures present the local vortex strength at the measurement/calculation plane.

The calculated vortex strength matches the wind tunnel test data over the complete set of conditions. The test data vortex strength is calculated from averaged vector maps, which may lead to a slight underestimation of the measured vortex strength.
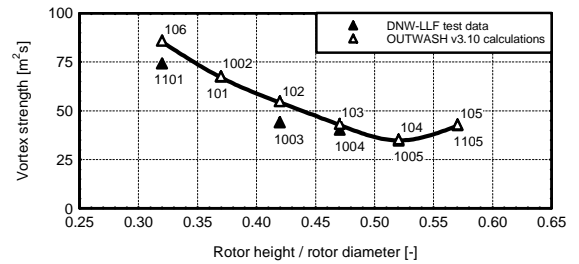

Figure 17 Ground vortex strength vs. rotor height comparison between OUTWASH code (improved model) and experimental data
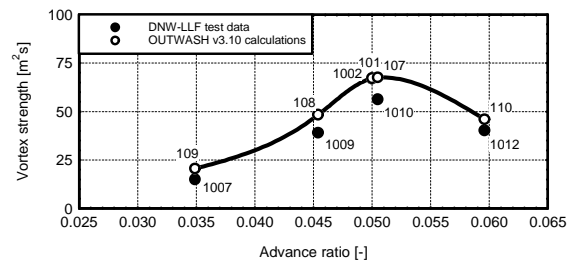

Figure 18 Ground vortex strength vs. advance ratio comparison between OUTWASH code (improved model) and experimental data

It is recommended to further validate the improved model with wind tunnel, or preferably, full scale test data. Measurements should at least be taken at both sides and upwind of the rotor. In this way the ground vortex position, complete shape, and the change of strength over the ground vortex can be measured.
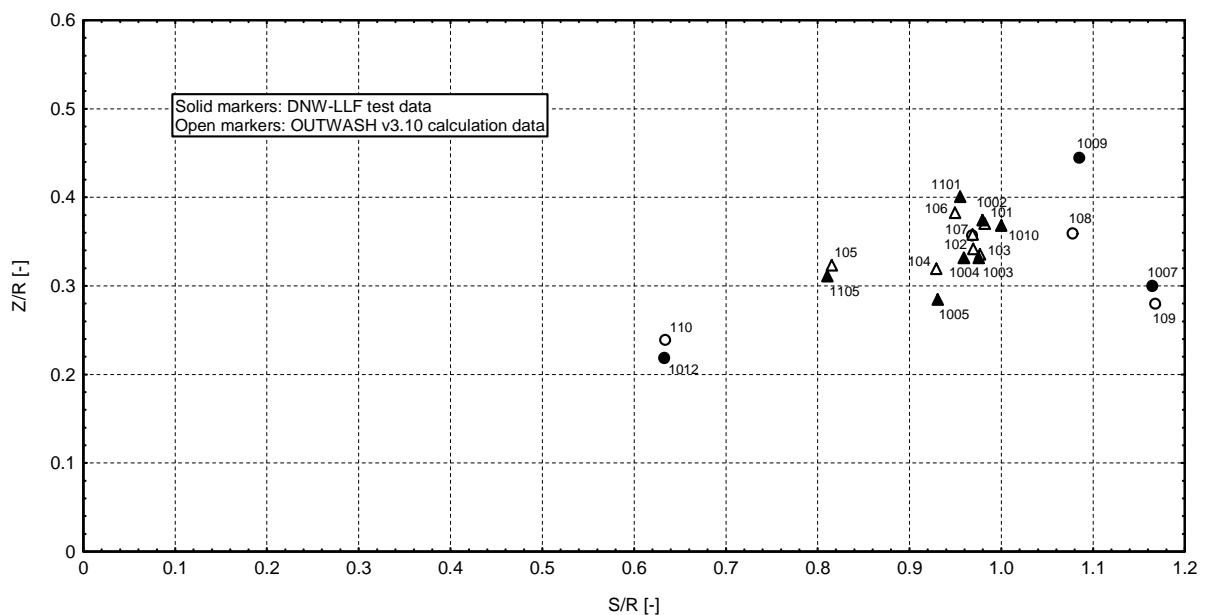

Figure 16 Comparison between OUTWASH (improved ground vortex model) and experimental results

Concluding remarks

In the 4th Framework project HELIFLOW, a wind tunnel test was performed in DNW's Large Low-speed Facility (LLF) using the DLR BO 105 powered wind tunnel model (scale 1:2.5). State of the art airflow test techniques as Laser Light Sheet (LLS) and Particle Image Velocimetry (PIV) were applied during testing to measure the flow phenomena of the ground vortex.

The test results included the effect of rotor height above ground and air velocity on the ground vortex core position and strength in the measurement plane, which were determined from the LLS-vector maps.

The theoretical assessment of the ground vortex was performed using a ground vortex model developed in-house by NLR. The model is part of the rotorwash induced horizontal airflow calculation tool OUTWASH. The OUTWASH code predicts the magnitude of the horizontal airflow over the ground caused by low-flying helicopters and the area that is affected by the helicopter outwash.

The OUTWASH code was used to refine the wind tunnel test matrix and to define the experimental set-up for the flow measurements to be executed. After the HELIFLOW wind tunnel tests were performed, the experimental results were used to improve the OUTWASH ground vortex position model. Calculation results from the improved OUTWASH ground vortex model show a very good match for all the HELIFLOW measurement conditions.

It is recommended to further validate the improved ground vortex model with more wind tunnel, or preferably, full-scale test data.

Acknowledgements

References

1. "Improved Experimental and Theoretical Tools for Helicopter Aeromechanic and Aeroacoustic Interactions", Acronym: HELIFLOW, Technical Annex to the Project Programme, Ottobrunn, 22 April 1996.
2. Boer, J.F.; Hoolhorst, A.; Stevens, J.M.G.F., "Mathematical modelling for helicopter outwash airflow" (In Dutch), NLR-CR-95664-L, July 1996.
3. Boer, J.F.; Hoolhorst, A.; Stevens, J.M.G.F., "Mathematical modelling for helicopter outwash airflow in conditions with a ground vortex" (In Dutch), NLR-CR-98032, January 1998.
4. Boer, J.F., "HELIFLOW Task 3 Ground Vortex pre-test calculations", NLR TR-98578 (HFLOW/3/NLR/01A), December 1998.
5. Pengel, K., "Report on particle image velocimetry data ", HFLOW/3/DNW/09, March 2001.
6. Boer, J.F., "HELIFLOW Task 3 Ground Vortex test results analysis", NLR TR-2001-246 (HFLOW/3/NLR/02A), June 2001.
7. Ferguson, S.W., "Rotorwash Analysis Handbook", Volume I – Development and Analysis, Federal Aviation Authorities, US Department of Transportation, DOT/FAA/RD-93/31,I, June 1994.
8. Sun, M., "A Study Of Helicopter Rotor Aerodynamics In Ground Effect At Low Speeds", Ph.D. Thesis, Princeton University, Department of Mechanical and Aerospace Engineering, October 1983.
9. Curtiss, H.C., Jr.; Sun, M.; Putman, W.F.; Hanker, E.J., Jr., "Rotor Aerodynamics in Ground Effect At Low Advance Ratios", Journal of the American Helicopter Society, No. 29-1, January 1984.
10. Sun, M.; Curtiss, H.C., Jr., "An Experimental Study Of Rotor Aerodynamics In Ground Effect At Low Speeds", Chinese Journal of Aeronautics, Vol. 3 No. 2, May 1990.